Polymer Chemistry

ROYAL SOCIETY OF CHEMISTRY

PAPER

View Article Online
View Journal

Cite this: DOI: 10.1039/d5py00224a

Received 4th March 2025,
Accepted 9th August 2025

DOI: 10.1039/d5py00224a

rsc.li/polymers

Homo(co)polymerization of bio-derived long alkyl chain methacrylate and methyl methacrylate using a readily accessible aminophosphine-based Lewis pair

Bingqi Wang,†[a] Zhen Wu,†[a] Yin Cai,[a] Fang Ge *[a] and Xiaowu Wang *[b]

Lewis pair polymerization (LPP), emerging as an effective polymerization method, has been broadly investigated and applied in the synthesis of diverse polymers, *e.g.* poly(meth)acrylates, polyesters, polyethers *etc.* In the Lewis pair-mediated polymerization of conjugated polar monomers, Lewis bases having P–N bonds showed great promise in mediating controlled/living (co)polymerization of short alkyl acylates and short alkyl methacrylates. However, there have been far fewer experimental studies on long alkyl chain acrylates or methyl acrylates using LPP. Introduction of long alkyl side chains offers the opportunity to explore their influence on the parameters of the generated materials and tune the physical properties of copolymers to cater to society's demands. In this contribution, we synthesized the new aminophosphine LB bis(*N*,*N*-diethylamino)methylphosphine [$(Et_2N)_2PMe$] *via* varying the number of P–N bonds, and combined it with $^iBu_3Al$ to form the Lewis pair (LP) for the (co)polymerization of methyl methacrylate (MMA) and bio-derived lauryl methacrylate (LMA). $(Et_2N)_2PMe/^iBu_3Al$ showed both controlled polymerization of MMA and LMA at a monomer/$(Et_2N)_2PMe$ molar ratio of 1600/1 or 700/1, respectively. Taking advantage of the linear chain end of PLMA, the block copolymer of PLMA-*b*-PMMA was synthesized *via* the sequential addition method and its physical properties were investigated.

Introduction

Poly(meth)acrylates are important materials in our daily life. They can be used as glue, lubricants, textiles, *etc.* The properties of homopoly(meth)acrylates, however, vary significantly depending on the structure of their alkoxyl side chains.[1] For example, the length of alkoxyl side chains will have a significant effect on the flexibility of the polymer.[2,3] The bio-sourced acrylate monomer, lauryl methacrylate (LMA), having a long alkoxyl group, has attracted our attention. The twelve-carbon long chain brings special properties to the homopolymer due to its superior hydrophobic properties and low glass transition temperature ($T_g \sim -65$ °C).[4,5] Therefore, LMA was used as a soft block in the synthesis of acrylic thermoplastic elastomers (TPE), and its hydrophobicity can also be used to construct various amphiphilic block copolymers.[6–8] Previously, homo(co)polymerization of LMA has been achieved by free radical polymerization,[4,9–12] anionic polymerization,[5,13–18] cationic polymerization,[19] and group transfer polymerization (GTP).[20–22] To the best of our knowledge, little is known about the polymerization of LMA using Lewis pair polymerization (LPP), which is an efficient polymerization method for the synthesis of poly(meth)acrylates. Among the reported Lewis bases (LBs), the phosphines containing the P–N bond exhibited excellent polymerization abilities. In 2021, Wang and co-workers reported the utilization of pyridinylidenaminophosphines (PYAPs) as Lewis bases and applied them in Lewis pair polymerization to controllably achieve PMMA.[23] Later in 2023, Zhang *et al.* elaborated the application of mono- or di-initiating pyridinylidenaminophosphines as LBs, which could produce well-defined multi-block biomass-derived acrylic copolymers *via* LPP from one-pot synthesis.[24] In the year 2024, Zhang and co-workers synthesized guanidine phosphine (NsI*t*Bu)PPh_2 and applied it as a Lewis base to synthesize poly(vinylpyridine) (PVP) based (co)polymers.[25]

We previously reported[26] the application of the commercially available tris(dimethylamino)phosphine (HMPT) featuring the P–N bond as a Lewis base (LB) paired with $^iBu_3Al$ to polymerize MMA. However, the HMPT-based LP system showed insufficient initiation efficiency and low polymerization degree in LMA. Preliminary results indicate that replacement of the dimethylamino group with the diethylamino group improves the initiation efficiency of LMA. This phenomenon indicates that the diethylamino group exhibits stronger steric hindrance effects and electronic modulation

---

[a] College of Chemistry and Chemical Engineering, 266071, Qingdao University, Qingdao, China. E-mail: gefang@qdu.edu.cn

[b] College of Chemical Engineering, Qingdao University of Science and Technology, Qingdao 266042, China. E-mail: wangxw@qust.edu.cn

† These authors contributed equally to this work and should be considered co-first authors.

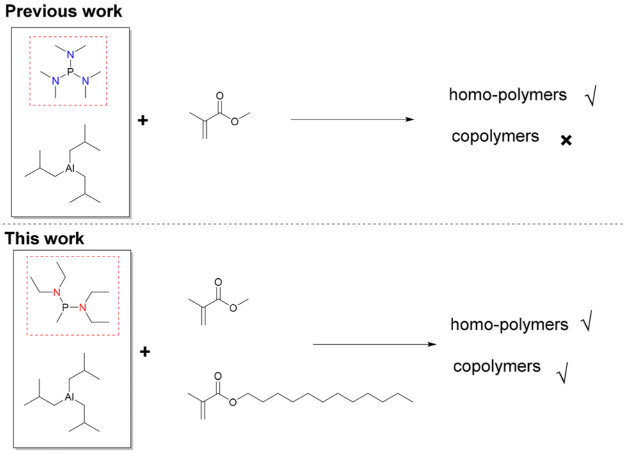

Fig. 1 Previous work and present work in this study.

capabilities than the dimethylamino group. The larger diethylamino substituent likely enhances the controllability of the polymerization by adjusting the stereochemical environment of the active center, which is reflected by increasing the stability of the active species through inter- or intramolecular ion pair interactions.[27,28]

To make progress in the use of aminophosphine-based Lewis pairs in the controlled synthesis of (meth)acrylate monomers and expand the diversity of polymers, a molecular engineering strategy was proposed to structurally modify tri(diethylamino)phosphine – retaining two diethylamino groups to maintain their fundamental performance while a third substituent was introduced on the P atom. This “dual diethylamino + variable substituent” design (*i.e.*, constructing $(Et_2N)_2PMe$, $(Et_2N)_2PPh$, and $(Et_2N)_2PCy$ compounds) preserves the inherent advantages of diethylamino groups while enabling fine-tuning of catalytic reactivity through the electronic/steric effects of the third substituent. Such an approach establishes a molecular design foundation for Lewis bases for achieving high and controlled (co)polymerization of LMA. Therefore, three new aminophosphines were synthesized by adjusting the number of P–N bonds and the steric hindrance/electronic effects of substituents on the P atom. Combining them with $^{i}Bu_3Al$ provided Lewis pairs for the (co)polymerization of MMA and LMA. Among these systems, the $(Et_2N)_2PMe/^{i}Bu_3Al$ Lewis pair showed high efficiency and controllability in the polymerization of LMA and block co-polymerization of LMA and MMA. This in turn afforded a convenient system to synthesize the block polymer of PLMA-*b*-PMMA (Fig. 1).

Results and discussion

Synthesis of aminophosphines and their applications in the LPPs of alkyl methacrylates

$(Et_2N)_2PMe$, $(Et_2N)_2PCy$ and $(Et_2N)_2PPh$ were synthesized *via* modified procedures (for details, please check the SI). To evaluate the performance of the synthesized aminophosphines in LP mediated polymerization, we combined them with different organoaluminum Lewis acids (LAs) [such as $(4\text{-Me-}2,6\text{-}^{t}Bu_2\text{-}C_6H_2O)_2AlMe$ ($MeAl(BHT)_2$), $^{i}BuAl(BHT)_2$, $^{i}Bu_2Al(BHT)$, and $^{i}Bu_3Al$] to achieve the polymerization of LMA. Control experiments showed that neither the aminophosphines nor organoaluminums can polymerize the LMA independently (Table S1). It is well-known that the matching of the acidity and steric effect of the LA to LB is important to realize controlled/living polymerization.[29] We first chose a Lewis acid with slightly higher Lewis acidity [$MeAl(BHT)_2$] compared with $(Et_2N)_2PMe$ to perform the polymerization of LMA at 25 °C (LMA/LB = 100/1, $[M]_0$ = 1.14 M). PLMA can be generated quantitatively within 40 min but with broad polydispersity ($Đ$ = 1.62) (Table S2, run 3). Then, the combination of $(Et_2N)_2PMe$ with the larger steric hindrance LA [$^{i}BuAl(BHT)_2$] can produce PLMA quantitatively, too. The generated PLMA has relatively small polydispersity ($Đ$ = 1.34) (Table S2, run 4). To improve the polymerization performance, we resorted to other organoaluminums, which have less steric hindrance and smaller/comparable acidity. Both $(Et_2N)_2PMe/^{i}Bu_2Al(BHT)$ and $(Et_2N)_2PMe/^{i}Bu_3Al$ systems produced PLMA quantitatively under the same reaction conditions (LMA/LB = 100/1, $[M]_0$ = 1.14 M). The GPC curve of the polymer generated from $(Et_2N)_2PMe/^{i}Bu_2Al(BHT)$ showed a unimodal distribution. The polymer showed a relatively small polydispersity ($Đ$ = 1.39) with M_n = 80.4 kg mol^{-1} (Table S2, run 5). There is a big discrepancy between M_n^{GPC} (80.4 kg mol^{-1}) and M_n^{calcd} (25.6 kg mol^{-1}), which is ascribed to the low initiation efficiency (I^* = 32%) (Table S2, run 5). Interestingly, GPC curves of the polymer obtained using $(Et_2N)_2PMe/^{i}Bu_3Al$ showed a unimodal distribution ($Đ$ = 1.14). The generated polymer had a molecular weight of 32.7 kg mol^{-1}, which is slightly higher than the calculated molecular weight, 25.6 kg mol^{-1} (Table S2, run 6). Moreover, a much higher initiation efficiency (I^* = 78%) was achieved when $^{i}Bu_3Al$ was used in combination with $(Et_2N)_2PMe$ (Table S2, run 6). Subsequently, we set $^{i}Bu_3Al$ as the optimal LA and combined it with $(Et_2N)_2PPh$ or $(Et_2N)_2PCy$ to find the best system for the (co)polymerization of LMA.

$(Et_2N)_2PPh$, and $(Et_2N)_2PCy$ were applied as LBs to polymerize LMA together with $^{i}Bu_3Al$. Experimental data revealed that under identical reaction conditions (LMA/LB = 100/1, $[M]_0$ = 1.14 M), these two systems can achieve quantitative polymerization of LMA within 40 min at 25 °C. Both $(Et_2N)_2PPh/^{i}Bu_3Al$ (I^* = 62%, Table S2, run 7) and $(Et_2N)_2PCy/^{i}Bu_3Al$ (I^* = 42%, Table S2, run 8) showed lower initiation efficiency than $(Et_2N)_2PMe/^{i}Bu_3Al$ (I^* = 78%). Moreover, the polydispersities of polymers obtained from $(Et_2N)_2PPh/^{i}Bu_3Al$ ($Đ$ = 1.35) and $(Et_2N)_2PCy/^{i}Bu_3Al$ ($Đ$ = 1.46) were much higher than that of $(Et_2N)_2PMe/^{i}Bu_3Al$ ($Đ$ = 1.14). These results indicate that $(Et_2N)_2PCy$ with the largest third substituent hinders the nucleophilicity of the phosphine center, which leads to the lowest polymerization efficiency and produces PLMA with much low initiation efficiency. In comparison, $(Et_2N)_2PMe$, having the smallest third substituent, achieved the highest initiation efficiency and better control of the molecular weight and narrow polydispersity of poly(LMA). Based on the above results, $(Et_2N)_2PMe/^iBu_3Al$ was selected as the optimal system for further investigation.

To show the capability of the $(Et_2N)_2PMe/^iBu_3Al$ system in achieving a wide range of molecular weights, we investigated the polymerization of LMA at various targeted degrees of polymerization (DP), from 30 to 1000. Varying the molar ratio of $[LMA]_0/[(Et_2N)_2PMe]_0$ with a DP ranging from 30 to 700 yielded quantitative conversion of LMA. Moreover, the GPC curves of the obtained polymers showed that the M_ns increased linearly, while the polydispersity remains narrow ($Đ$ = 1.12–1.36) (Table 1, runs 1–4, Fig. 2a and b).

Moreover, a kinetic experiment was performed at $[LMA]_0/[(Et_2N)_2PMe]_0 = 300/1$; an aliquot was taken from the reaction mixture and analysed by NMR spectroscopy and GPC analysis. The GPC curves of these PLMA samples gradually shifted to the higher molecular weight region with PLMA conversion increasing (Fig. S9). The plot of the M_ns of PLMA *vs.* LMA conversions fitted a linear line with excellent linearity ($R^2 = 0.994$) (Fig. S10). Moreover, the generated PLMA in each aliquot maintained narrow $Đ$s in the entire polymerization process ($Đ$ = 1.16–1.26) (Table S3, runs 1–5). And the plot of monomer conversion *vs.* reaction time also gave a linear increasing (R^2 = 0.998) relationship (Fig. S11). The reaction was completed within 6 min. These results indicated that the $(Et_2N)_2PMe/^iBu_3Al$ system can polymerize LMA in a controlled manner. The deviation between M_n^{GPC} and M_n^{calcd} (DP = 100–700) might be due to the application of PMMA standard samples in GPC analysis. In order to verify this speculation, the M_n^{NMR} was determined from the ^1H NMR of the polymer ($[LMA]_0/[LB]_0 = 10/1$) (see Fig. S29 and Table S6). By the integration of the $\mathbf{CH_2}$–N moiety (2.88–3.17 ppm) from the terminal group (from LB) of the polymer chain and the $\mathbf{CH_2}$–O moiety (3.91 ppm) from repeat units of PLMA, we calculated the average degree of polymerization ($\overline{DP_n}$) of PLMA and obtained its M_n^{NMR}, which is smaller than the M_n^{GPC} (see Table S6; for the calculation details, please see the SI). A further increase of the DP to 1000 resulted in incomplete monomer conversion (52%) (Table 1, run 5), which might be due to the deactivation of the active species under such high monomer loading.[20]

To verify the chain-end group fidelity of the obtained PLMA, the MALDI-TOF-MS spectrum of low-M_W PLMA was recorded. The spectrum showed only one population of the molecular ion peak. It features the linear PLMA chain capped with $(Et_2N)_2PMe$ and H chain ends, which indicates that the polymer chain is without back-biting (Fig. 2c).

Then, we sought to assess the versatility of $(Et_2N)_2PMe/^iBu_3Al$ LP for other monomers, such as MMA. Varying the molar ratio of $[MMA]_0/[(Et_2N)_2PMe]_0$ with a DP ranging from 200 to 1600 yielded quantitative conversions. The GPC curves of the generated polymethylmethacrylates (PMMAs) showed a linear increase of M_ns (20.1–151.7 kg mol^{-1}), which coincided well with the theoretical value. The polydispersity of the obtained polymers showed narrow $Đ$s (1.13–1.24) (Table 1, runs 7–10, Fig. S12 and S13). These results indicated that the $(Et_2N)_2PMe/^iBu_3Al$ system can polymerize MMA in a controlled manner.

To clarify the end-cap of the PMMA generated from the $(Et_2N)_2PMe/^iBu_3Al$ system, PMMA with a molecular weight of 10.2 kg mol^{-1} was analysed (sample obtained from run 11, Table 1). The spectrum showed two populations of molecular ion peaks. The major population features the linear PMMA chain capped with $(Et_2N)_2PMe$ and the cyclic β-ketoester or δ-valerolactone chain ends, where $(Et_2N)_2PMe$ was derived from the chain initiation by $(Et_2N)_2PMe$ (190.27), and the cyclic chain end [100.12 (MMA) − 31.03 (loss of MeO) = 69.09] was derived from the back-biting reaction (Fig. S14).[29] The minor population of peaks revealed a PMMA linear chain end capped with $(Et_2N)_2PMe$ without back-biting. These results were quite different from our previous work, in which the chain end of the PMMA produced from the $HMPT/^iBu_3Al$ system was mainly the back-biting chain end capped with HMPT and cyclic β-ketoester or δ-valerolactone (Fig. S15).

Table 1 The results of polymerization of LMA and MMA *via* the $(Et_2N)_2PMe/^iBu_3Al$ system

Run[a]	LB/LA/M	Conv.[b] [%]	Time [min]	M_n^{GPC} [c] [kg mol^{-1}]	M_n^{calcd} [d] [kg mol^{-1}]	$Đ$[c]	I^*[d] [%]
1	1/2/30 LMA	>99	30	22.3	7.8	1.36	35
2	1/2/100 LMA	>99	40	32.7	25.6	1.14	78
3	1/2/300 LMA	>99	120	92.2	76.5	1.17	83
4	1/4/700 LMA	>99	280	240.3	178.3	1.12	74
5	1/8/1000 LMA	52	360	—	—	—	—
6[e]	1/2/30 LMA	—	3 s	18.9	—	1.20	—
7	1/2/200 MMA	>99	80	32.9	20.2	1.13	61
8	1/2/400 MMA	>99	180	54.0	40.2	1.14	74
9	1/4/800 MMA	>99	300	92.4	80.3	1.23	87
10	1/8/1600 MMA	>99	420	151.7	160.4	1.24	106
11[e]	1/2/200 MMA	—	5 s	13.1	—	1.20	—

[a] Conditions: the polymerization reaction was performed at ambient temperature in a predetermined amount of toluene using the following procedure: $[LMA]_0$ = 1.14 M, $[MMA]_0$ = 3.0 M. [b] Monomer conversion measured by ^1H NMR. [c] M_n^{GPC} and $Đ$ were determined by gel permeation chromatography relative to the PMMA standard in THF. [d] Initiation efficiency (I^*) = M_n^{calcd}/M_n^{GPC}, where $M_n^{calcd} = [M_W(M)] \times ([M]_0/[LB]_0)$ (conversion %) + M_W of chain-end groups. [e] After the sample was mixed, it was quickly quenched in the middle of the reaction. Samples were used to test MALDI-TOF MS.

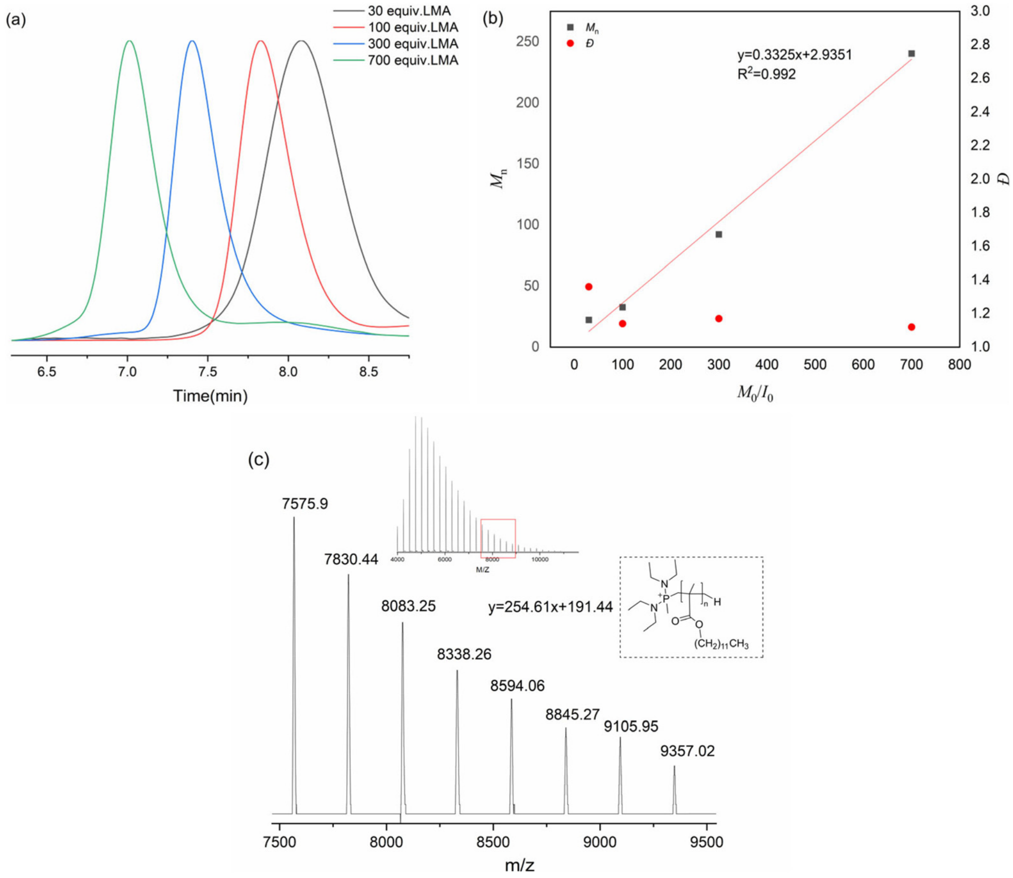

Fig. 2 (a) GPC curves of the obtained PLMA at different monomer ratios (sample obtained from runs 1–4, Table 1). (b) Plots of M_n and $Đ$ for the obtained PLMA *versus* $[LMA]_0/[(Et_2N)_2PMe]_0/[^iBu_3Al]_0$ ratios (sample obtained from runs 1–4, Table 1). (c) MALDI-TOF-MS spectrum of the low-M_W PLMA sample produced using $[(Et_2N)_2PMe]_0/^iBu_3Al$ in toluene at ambient temperature (sample obtained from run 6, Table 1, M_n = 18.9 kg mol^{-1}, $Đ$ = 1.20).

Since the $(Et_2N)_2PMe/^iBu_3Al$ Lewis pair could achieve PLMA with a linear PLMA chain end without back-biting, we therefore explored the possibility of synthesizing PLMA-based block copolymers. Before we performed the polymerizations to synthesize PLMA-based block copolymers, we first conducted chain extension experiments to provide evidence of the living chain end characteristic of $(Et_2N)_2PMe/^iBu_3Al$ in the polymerization of LMA. After polymerization of the first batch of LMA (200 equiv.) was complete (M_n = 59.8 kg mol^{-1}, $Đ$ = 1.22), a second batch of LMA (200 equiv.) was added (Table S4, run 1). The GPC curve of the generated PLMA shifted to higher molecular weight (M_n = 121.6 kg mol^{-1}) with a relatively narrow $Đ$ = 1.24 (Fig. S16).

Investigation of the mechanism

To gain further insights into the polymerization behaviour, the interaction of LB and LA was measured by the NMR technique (Fig. S17 and S18). The chemical resonance of free $(Et_2N)_2PMe$ (79.5 ppm) in ^{31}P NMR was shifted to 68.5 ppm after mixing with an equal molar amount of $^iBu_3Al$ (Fig. S17), which indicates the formation of the classical Lewis acid/base adducts (CLA). After the addition of an equal equivalent of LMA into the CLA solution, dissociation of the $(Et_2N)_2PMe/^iBu_3Al$ adduct was observed. The ^{31}P NMR spectrum shows two peaks. The broad one at 68.5 ppm correlates to the chemical shift of $(Et_2N)_2PMe$ in CLA. Another peak at 61.1 ppm is assigned to the zwitterionic active species. These two species have the ratio of 84.7% (68.5 ppm)/15.3% (61.1 ppm) (Fig. S18). The *in situ* NMR experiments indicated that CLA did not dissociate completely in the presence of an equal amount of LMA, which might explain the insufficient initiation at the initial stage of the reaction, thus resulting in a moderate initiation efficiency (DP = 100–700) and low initiation efficiency (DP < 100) of the $(Et_2N)_2PMe/^iBu_3Al$ system.

It is well known that the electronic and the stereochemical environment of the active center can reflect the stability and reactivity of the active species through inter- or intramolecular ion pair interactions.[27,28] This conclusion could be clearly drawn from the data in Table S2. The structure of the LB and the good adjustment between the LB and LA lead to different polymerization results. The stronger steric hindrance effects and electronic modulation capabilities of $(Et_2N)_2PMe$ endowed it with suitable nucleophilicity and enhanced the stability of the active species. But besides the factors we discussed above, the

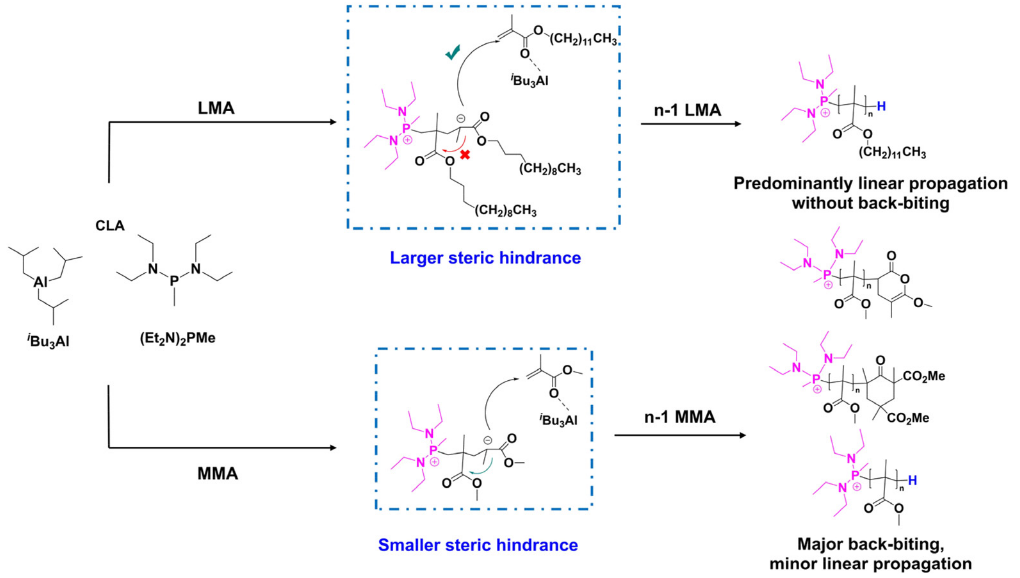

Fig. 3 The proposed mechanism.

structure of the monomer also plays an important role. The back-biting side reaction in MMA polymerization was reduced compared to our former HMPT/^{i}Bu$_3$Al system (Fig. S15), but still existed in PMMA synthesis *via* the (Et$_2$N)$_2$PMe/^{i}Bu$_3$Al system. However, the back-biting side reaction vanished when we used LMA as the monomer. The long alkoxyl side chains in LMA acted as a shield to effectively protect/stabilize the active species and block the back-biting side reaction (Fig. 3).

PLMA-based copolymer syntheses mediated by the (Et$_2$N)$_2$PMe/^{i}Bu$_3$Al system

After demonstrating the success of the (Et$_2$N)$_2$PMe/^{i}Bu$_3$Al system in the controlled polymerization of MMA and LMA, we attempted to synthesize copolymers by the copolymerization of MMA with LMA.

First, the copolymerization was performed using the LMA/MMA mixture ([LMA]$_0$/[MMA]$_0$ = 100/100) in a one-pot manner at 25 °C. The polymer was obtained quantitatively with M_n^{GPC} = 52.1 kg mol^{-1} and $Đ$ = 1.21 (Table 2, run 1, and Fig. S19). In order to further investigate the copolymerization reaction of MMA/LMA and clarify the construction of the copolymer, we monitored the copolymerization reaction by ^{1}H NMR spectroscopy at a periodic time intervals and constructed kinetic curves of the polymerization rate. As shown in Fig. S20 and Table S5, the conversion of these two monomers took place at the same time, and the propagation rate of MMA is nearly the same as that of LMA throughout the whole propagation process. Based on these data, the copolymer produced from the one-pot copolymerization reaction of the mixture of LMA and MMA is an alternative copolymer. In order to verify this conclusion, we also recorded the ^{13}C NMR spectra of (co)polymers (PMMA, PLMA, PLMA-*alt*-PMMA and PLMA-*b*-PMMA). As shown in Fig. S21, the chemical shifts of the α-C and β-C were 45.0 ppm/44.7 ppm from PMMA and 45.2 ppm/44.8 ppm from PLMA (see Fig. S22). As for the block copolymer PLMA-*b*-PMMA (see Fig. S22 Q2), two sets of α-C and β-C signals were observed, which were in agreement with the chemical shifts of α-C and β-C from PMMA and PLMA. This indicated the existence of -(-MMA-MMA-)$_n$- and -(-LMA-LMA-)$_m$- blocks (PMMA and PLMA) in the copolymer chain. But the special chemical shifts of α-C and β-C from -LMA-MMA- were difficult to observe due to the overlapping and weak resonance compared to the α-C and β-C signals of the repeating units from the PMMA block and the PLMA block. As for PLMA-*alt*-PMMA, it shows

Table 2 The results of copolymerization of MMA and LMA using the (Et$_2$N)$_2$PMe/^{i}Bu$_3$Al system

Run^a	Monomer MMA/LMA	Conv.^{b} [%]	Time [min]	$M_n^{GPC\ c}$ [kg mol^{-1}]	$M_n^{calcd\ d}$ [kg mol^{-1}]	$Đ^c$	I^{*d} [%]
1	100/100	>99	180	52.1	35.6	1.21	68
2^{1st}	0/100	>99	3	30.3	25.6	1.21	84
2^{2nd}	100/100	>99	180	41.9	35.6	1.22	85

^{a} Conditions: the polymerization reaction was performed at ambient temperature in a predetermined amount of toluene using the following steps: for LB/2LA/M, [LMA]$_0$ = 1.14 M, [MMA]$_0$ = 3.0 M. ^{b} Monomer conversion measured by ^{1}H NMR. ^{c} M_n^{GPC} and $Đ$ were determined by gel permeation chromatography relative to the PMMA standard in THF. ^{d} Initiation efficiency (I^*) = M_n^{calcd}/M_n^{GPC}, where M_n^{calcd}= [M_W(M)] × ([M]$_0$/[LB]$_0$)(conversion %) + M_W of chain-end groups.

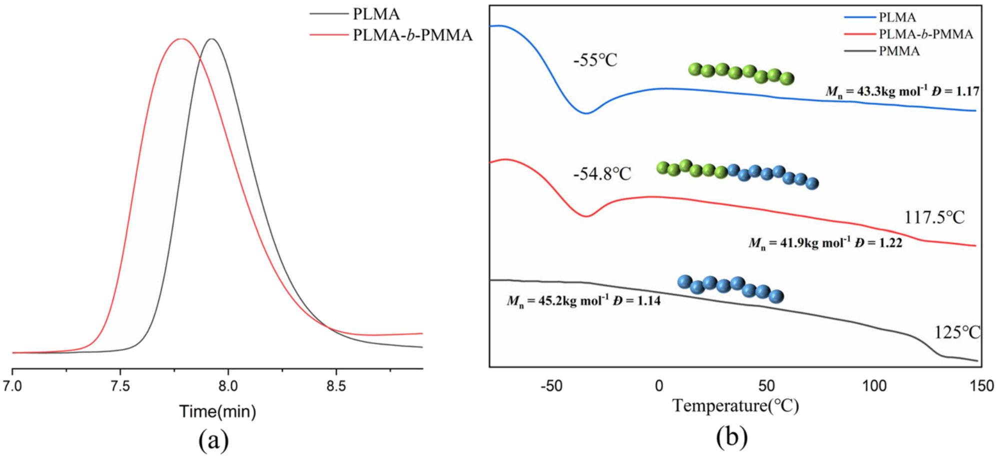

Fig. 4 (a) GPC traces of the produced copolymer from MMA and LMA using the $(Et_2N)_2PMe/{}^iBu_3Al$ system (sample obtained from run 2, Table 2). (b) DSC curves of PMMA (M_n = 45.2 kg mol^{-1}, Đ = 1.14) and PLMA (M_n = 43.3 kg mol^{-1}, Đ = 1.17) homopolymers as well as block copolymers (sample obtained from run 2, Table 2).

two sets of chemical shifts of α-C and β-C, which are different from the chemical shifts of α-C and β-C in PLMA-*b*-PMMA, PMMA and PLMA (see Fig. S22 Q1). This indicates the existence of unique repeating units, which presents as -(-MMA-LMA-)$_n$- in the copolymer. And this also proved that the structure of the copolymer is PLMA-*alt*-PMMA. Differential scanning calorimetry (DSC) analysis of the copolymer shows only one glass transition temperature (T_g = 0 °C), which lies in between the glass transition temperatures of the parent homopolymers [PLMA (T_g = −55 °C) and PMMA (T_g = 125 °C)] (Fig. S23). This result further indicated that the polymer obtained from this reaction is a copolymer but not the mixture of two homopolymers PMMA and PLMA.

Later, we tried to synthesize the block copolymer *via* the sequential addition method of LMA and MMA (LMA/MMA = 100/100). After complete consumption of 100 equiv. of LMA (M_n^{GPC} = 30.3 kg mol^{-1}, Đ = 1.21), MMA was added and the polymerization was maintained until all the MMA was consumed, which afforded the block copolymer (M_n^{GPC} = 41.9 kg mol^{-1} and Đ = 1.22) (Table 2, run 2, Fig. 4a). The PLMA-*b*-PMMA copolymer shows a unimodal distribution in GPC analysis and the M_n increased along with the addition of MMA. The DSC analysis of the copolymer shows two glass transition temperatures (${T_g}^1$ = −54.8 °C; ${T_g}^2$ = 117.5 °C) which were close to the glass transition temperatures of PLMA (T_g = −55.0 °C) and PMMA (T_g = 125.0 °C) (Fig. 4b). These results indicate that the obtained copolymer is a well-defined block copolymer rather than a random copolymer or a mixture of PMMA and PLMA.

Conclusions

In summary, we synthesized a new aminophosphine, namely, $(Et_2N)_2PMe$, by adjusting the number of P–N bonds and the steric hindrance of alkyl groups on N and P atoms. Then, $(Et_2N)_2PMe$ was treated as an LB and combined with ${}^iBu_3Al$ to construct an LP. MMA and bio-derived long alkyl chain methacrylate—lauryl methacrylate (LMA)—were (co)polymerized *via* the $(Et_2N)_2PMe/{}^iBu_3Al$ system. The degree of polymerization is up to 1600 for MMA and 700 for LMA. PLMA-*b*-PMMA was synthesized and characterized. The $(Et_2N)_2PMe/{}^iBu_3Al$ system remedies the defect of our previous work ($HMPT/{}^iBu_3Al$ system), which can only conduct the (co)polymerization of short alkyl acrylates and short alkyl methacrylate. Besides that, the $(Et_2N)_2PMe/{}^iBu_3Al$ system showed the ability to polymerize the long alkyl chain monomer LMA, which has not been used as monomer for the investigation of the polymerization reaction *via* LPP. This provided more choices to synthesize polymers with long alkyl side chains, which would in turn offer the opportunity to explore their influence on the parameters of basic materials and tune the physical properties of copolymers to cater to society's demands. Other aminophosphines are under investigation to broaden the categories of conjugated polar monomers and will be reported in due course.

Author contributions

F. Ge and X. Wang conceived and designed the experiments; B. Wang and Z. Wu carried out the actual experiments and interpreted the data; Y. Cai assisted in performing the experiments. F. Ge and X. Wang wrote the manuscript.

Conflicts of interest

There are no conflicts to declare.

Data availability

Supplementary Information is available and contains detailed experimental procedures, characterization data, supplementary figures and tables. The data supporting this article have been included as part of the SI. See DOI: **https://doi.org/10.1039/d5py00224a**.

Acknowledgements

This work was supported by the National Natural Science Foundation of China (No. 21801148), the Shandong Provincial Natural Science Foundation, China (ZR2019BB020) and the financial support from Qingdao Sanli Benzo Chemical Industry Co., Ltd.

References

1 F. Fleischhaker, A. P. Haehnel, A. M. Misske, M. Blanchot, S. Haremza and C. Barner-Kowollik, *Macromol. Chem. Phys.*, 2014, **215**, 1192–1200.
2 Z. Czech, K. Agnieszka, P. Ragańska and A. Antosik, *J. Therm. Anal. Calorim.*, 2015, **119**, 1157–1161.
3 I. K. Varma, M. Patnaik and V. Choudhary, *J. Therm. Anal.*, 1990, **36**, 617–628.
4 H. Ahmad, M. Abu-Waesmin, M. M. Rahman, M. A. Jalil Miah and K. Tauer, *J. Appl. Polym. Sci.*, 2013, **127**, 620–627.
5 O. Nakagawa, N. Fujimoto, T. Nishiura, T. Kitayama and K. Hatada, *Polym. Bull.*, 1992, **29**, 579–586.
6 H. Zhang, H. Sun, X. Wang and Z. Wang, *ACS Appl. Polym. Mater.*, 2024, **6**, 6561–6571.
7 F. Boscán, M. Paulis and M. J. Barandiaran, *Eur. Polym. J.*, 2017, **93**, 44–52.
8 Q. Xu, L. Wang, F. Fu and X. Liu, *Prog. Org. Coat.*, 2020, **148**, 105884.
9 G. Patias, A. M. Wemyss, S. Efstathiou, J. S. Town, C. J. Atkins, A. Shegiwal, R. Whitfield and D. M. Haddleton, *Polym. Chem.*, 2019, **10**, 6447–6455.
10 J. Yu, C. Xu, X. Song, C. Lu, C. Wang, J. Wang and F. Chu, *Ind. Crops Prod.*, 2021, **168**, 113610.
11 W. Xu, X. Zhu, Z. Cheng and J. Chen, *J. Appl. Polym. Sci.*, 2003, **90**, 1117–1125.
12 C. György, C. Verity, T. J. Neal, M. J. Rymaruk, E. J. Cornel, T. Smith, D. J. Growney and S. P. Armes, *Macromolecules*, 2021, **54**, 9496–9509.
13 D. M. Haddleton, A. V. G. Muir, J. P. O'Donnell, S. N. Richards and D. L. Twose, *Macromol. Symp.*, 1995, **91**, 93–105.
14 T. Zhang, A. Zheng, G. Zou, D. Wei, X. Xu and Y. Guan, *Macromol. Chem. Phys.*, 2019, **220**, 1900390.
15 H. Sugimoto, M. Kuroki, T. Watanabe, C. Kawamura, T. Aida and S. Inoue, *Macromolecules*, 1993, **26**, 3403–3410.
16 B. C. Anderson, G. D. Andrews, P. Arthur Jr., H. W. Jacobson, L. R. Melby, A. J. Playtis and W. H. Sharkey, *Macromolecules*, 1981, **14**, 1599–1601.
17 V. Raghunadh, D. Baskaran and S. Sivaram, *J. Polym. Sci., Part A: Polym. Chem.*, 2004, **42**, 875–882.
18 M. K. Mishra, J. Bradley, R. G. Saxton and A. Duggal, *J. Polym. Sci., Part A: Polym. Chem.*, 2001, **39**, 947–950.
19 A. Fajrin, S. D. Marliana and D. S. Handayani, *IOP Conf. Ser.: Mater. Sci. Eng.*, 2018, **349**, 012003.
20 B. Sannigrahi, P. P. Wadgaonkar, J. C. Sehra and S. Sivaram, *J. Polym. Sci., Part A: Polym. Chem.*, 1997, **35**, 1999–2007.
21 A. Stiti, A. M. Cenacchi Pereira, G. Fleury, S. Lecommandoux and D. Taton, *Macromolecules*, 2024, **57**, 1713–1724.
22 D. Y. Sogah, W. R. Hertler, O. W. Webster and G. M. Cohen, *Macromolecules*, 1987, **20**, 1473–1488.
23 F. Ge, S. Li, Z. Wang, W. Zhang and X. Wang, *Polym. Chem.*, 2021, **12**, 4226–4234.
24 Y. Wan, J. He and Y. Zhang, *Angew. Chem., Int. Ed.*, 2023, **62**, e202218248.
25 Q. Ding, W. Zhao, F. Li, J. He and Y. Zhang, *Sci. China: Chem.*, 2024, **67**, 2737–2746.
26 Y. Cai, X. Zhao, B. Wang, W. Shi, F. Ge and X. Wang, *Macromol. Chem. Phys.*, 2024, **225**, 2300419.
27 M. Hong, J. Chen and E. Y. X. Chen, *Chem. Rev.*, 2018, **118**, 10551–10616.
28 M. L. McGraw and E. Y. X. Chen, *Macromolecules*, 2020, **53**, 6102–6122.
29 Q. Wang, W. Zhao, S. Zhang, J. He, Y. Zhang and E. Y. X. Chen, *ACS Catal.*, 2018, **8**, 3571–3578.